

Kinetic and Pharmacological Properties of the Sodium Channel of Frog Skeletal Muscle

DONALD T. CAMPBELL and BERTIL HILLE

From the Department of Physiology and Biophysics, University of Washington School of Medicine, Seattle, Washington 98195. Dr. Campbell's present address is the Department of Physiology, Yale University School of Medicine, New Haven, Connecticut 06510.

ABSTRACT Na channels of frog skeletal muscle are studied under voltage clamp and their properties compared with those of frog myelinated nerve. A standard mathematical model is fitted to the sodium currents measured in nerve and in muscle to obtain a quantitative description of the gating kinetics. At 5°C the kinetics in frog nerve and skeletal muscle are similar except that activation proceeds five times faster in nerve. Block of Na channels by saxitoxin is measured in nerve and in muscle. The apparent dissociation constants for the inhibitory complex are about 1 nM and not significantly different in nerve and muscle. Block of Na channels by external protons in muscle is found to have an apparent pK_a of 5.33 and a voltage dependence corresponding to action of 27% of the membrane potential drop. Both values are like those for nerve. Shift of the peak sodium permeability-membrane potential curve with changes of external pH and Ca^{++} are found to be the same in nerve and muscle. It is concluded that Na channels of nerve and muscle are nearly the same.

INTRODUCTION

This paper examines properties of the Na channel of frog muscle membranes under voltage clamp conditions. The guiding question to ask is if the Na channel of muscle is similar to that of nerves taken from the same species. For this reason the focus is on properties already well described in frog myelinated nerve. These include the kinetics of opening and closing of channels, the affinity of channels for saxitoxin and H^+ ions, and shifts of gating as the external concentration of Ca^{++} and H^+ ions is varied. The results show an overwhelming similarity in the two tissues, and we conclude that the channels may comprise the same molecular species.

METHODS

The experiments were done on fiber fragments from the semitendinosus muscle of the frog *Rana pipiens*, prepared and placed under voltage clamp by the method given in the first paper (Hille and Campbell, 1976). The notation of that paper is used here.

The object of the first series of experiments to be described was to measure the rates of activation and inactivation of Na channels under voltage clamp in order to develop a mathematical description of gating kinetics in muscle. The empirical kinetic model used follows the approach originated by Hodgkin and Huxley (1952) and applied by Adrian et

al. (1970) and Ildefonse and Roy (1972) to sodium currents of frog skeletal muscle. The time-course of sodium currents is represented by

$$I_{\text{Na}}(t, E) = [m(t, E)]^3 [h(t, E)] \bar{I}_{\text{Na}}(E), \quad (1)$$

where m and h are parameters ranging from zero to one and \bar{I}_{Na} is the hypothetical current-voltage relation that would obtain if m and h were simultaneously equal to one. Changes of m and h are governed by first-order transitions

$$\frac{dm}{dt} = \alpha_m(1 - m) - \beta_m(m), \quad (2)$$

$$\frac{dh}{dt} = \alpha_h(1 - h) - \beta_h(h), \quad (3)$$

with practical parameters m_∞ , τ_m , h_∞ , and τ_h defined by

$$m_\infty = \alpha_m / (\alpha_m + \beta_m), \quad (4)$$

$$\tau_m = 1 / (\alpha_m + \beta_m), \quad (5)$$

$$h_\infty = \alpha_h / (\alpha_h + \beta_h), \quad (6)$$

$$\tau_h = 1 / (\alpha_h + \beta_h). \quad (7)$$

Finally the voltage dependence of the rate constants is represented by empirical functions of the form used by Adrian et al. (1970):

$$\alpha_m = \frac{\bar{\alpha}_m (E - \bar{E}_m)}{1 - \exp [-(\bar{E}_m - E)/V_{\alpha m}]}, \quad (8)$$

$$= \bar{\beta}_m \exp [(\bar{E}_m - E)/V_{\beta m}], \quad (9)$$

$$= \bar{\alpha}_h \exp [(\bar{E}_h - E)/V_{\alpha h}], \quad (10)$$

$$\beta_h = \frac{\bar{\beta}_h}{1 + \exp [(\bar{E}_h - E)/V_{\beta h}]}. \quad (11)$$

Membrane currents for the kinetic experiments were recorded on-line with a minicomputer kindly built for us by Dr. T. H. Kehl and his staff (Kehl et al., 1975). All the refinements of the voltage clamp reported before were used in these studies, e.g., R_s compensation, Z_{ED} compensation, leak and capacity subtraction, etc. Membrane currents were sampled every 30 μs and recorded on digital magnetic tape. Then sodium currents during depolarizing test pulses were fitted to the following formula, simplified from Eqs. 1-7

$$I_{\text{Na}}(t) = A(1 - e^{-t/\tau_m})^3 e^{-t/\tau_h}, \quad (12)$$

where A is an amplitude factor. The equation assumes that m at the beginning of the test pulse is zero, a very good assumption, and that h inactivates fully to zero in the steady state, a less perfect assumption. A computer program in BASIC selected values of A , τ_m , and τ_h to minimize the sum of the squared differences between the observations and Eq. 12 using the Patternsearch routine (Colquhoun, 1971, p. 263) for minimization. As is described in the Results section, appropriate values for the constants in Eqs. 9-11 were then chosen to describe the voltage dependence of τ_m , τ_h , the peak sodium current, and h_∞ measured using various prepulses.

A second series of experiments was designed to measure the block of Na channels by externally applied saxitoxin. The solutions contained 0, 0.5, and 2.0 nM saxitoxin, 50 mM

tetraethylammonium chloride, 60 mM NaCl, 2 mM CaCl_2 , and 6 mM tris(hydroxymethyl)aminomethane buffer at pH 7.4. The saxitoxin was kindly provided by Dr. E. J. Schantz.

A third series of experiments was designed to measure the effects of H^+ ions and Ca^{++} ions on the voltage dependence and amplitude of peak sodium permeability. Bathing solutions were of two types. One had a fixed pH of 7.4 and five concentrations of Ca^{++} : 0, 0.5, 2, 5, and 20 mM. The other had a fixed 2 mM Ca^{++} and five pH values: 4.5, 5.2, 6.0, 7.4, and 9.4. The low pH buffer was piperazine + propionic acid, the neutral buffer was tris(hydroxymethyl)aminomethane + HCl, and the high pH buffer was tris(hydroxymethyl)aminomethane + cyclohexylaminopropanesulfonic acid. All solutions contained 60 mM NaCl, 50 mM tetraethylammonium chloride, and 10 mM buffer in addition to CaCl_2 . Sodium concentration was kept low to reduce errors from large currents flowing in the extracellular series resistance, since this series of experiments was done before the series resistance compensator had been developed. All test depolarizing steps were preceded by 60-ms 45-mV hyperpolarizations to reduce ordinary sodium inactivation. The holding potential was also increased in low-calcium solutions to avoid the effects of long-term sodium inactivation. Potentials were corrected for junction potentials. As described by Hille et al. (1975), peak sodium permeability was calculated from Na currents with the Goldman (1943) and Hodgkin and Katz (1949) equation, and the changes of peak P_{Na} versus E curves were analyzed by the model of Woodhull (1973) as described later.

RESULTS

Gating in Na Channels of Muscle

The time-course of sodium currents under voltage clamp was measured in several muscle fibers at 5°C. A partial family of currents from the most extensively studied fiber is shown in Fig. 1 on two time scales. The traces are drawn by computer from digitized on-line recordings after automatic subtraction of leakage and capacity currents. The time constants τ_m and τ_h and the steady-state values of m and h were then calculated in order to develop a complete kinetic model for sodium permeability changes in muscle. The stepwise determination of the required parameters is now described.

INACTIVATION OF NA CHANNELS The voltage dependence of h_∞ was determined by measuring the effect of various 200-ms conditioning prepulses on the peak sodium current elicited in a test pulse to near 0 mV. Results from three muscle fibers are plotted as symbols in Fig. 2 A. At the holding potential of -90 mV sodium channels are 10–30% inactivated and the potential for half inactivation is between -75 and -84 mV. The smooth curve is drawn from the kinetic model described later.

Eq. 12 was fitted to the first 100–200 points (3.0–6.0 ms) of the digitized voltage clamp currents to determine the Hodgkin-Huxley time constants τ_m and τ_h for activation and inactivation of sodium channels. In general the fit to Eq. 12 was very good with a standard deviation of the points from the fitted curve of less than 5% of the peak amplitude. A modification of Eq. 12 including a factor for incomplete sodium inactivation was also fitted to the observations to test if inactivation was incomplete for large depolarizations as reported by Ildefonse and Roy (1972). For steps to absolute potentials between -10 and +130 mV the

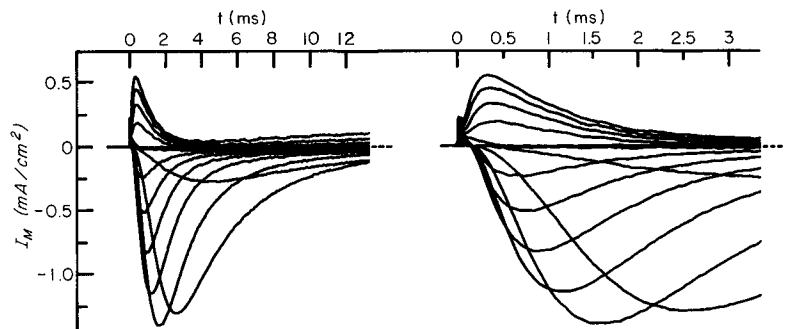


FIGURE 1. Time-course of sodium currents in a semitendinosus muscle fiber under voltage clamp at 5°C. The fiber was held at -90 mV, stepped to a prepulse of -135 mV for 50 ms, and then stepped to test pulse potentials ranging from -75 to $+120$ mV. Membrane currents corrected for leakage, capacity, and the impedance Z_{ED} were sampled on-line digitally every $30 \mu\text{s}$ and drawn later by computer on two time scales. The currents are small. Records taken earlier on the same fiber gave currents twice as large. Ends of fiber cut in 120 mM CsF. Outside bathed in standard frog Ringer solution. Voltage clamp was compensated for series resistance with a setting of 0.07. Experiment of 12/6/74.

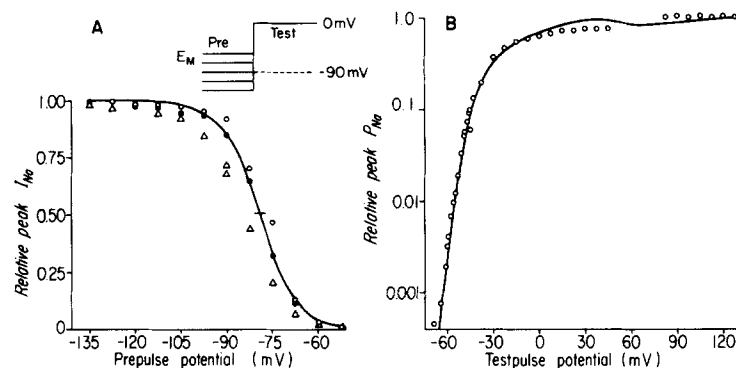


FIGURE 2. Observed and calculated $h_{\infty}E$ and $P_{Na}E$ curves. (A) Symbols are relative amplitude of peak sodium current measured at 0 mV after different 200-ms prepulses. Data from three fibers. Smooth curve calculated from Eqs. 4, 8, and 9. (B) Symbols are relative peak P_{Na} for currents of the fiber shown in Fig. 1. Smooth line is theoretical peak P_{Na} curve calculated from the complete voltage clamp model. At 0 mV the calculated value of m^3h in the model is 0.21. The inflections between 30 and 90 mV come from the factor W (Eq. 14).

best fitting curves never had more than 4% residual sodium current in the steady state, a value that may not differ significantly from zero in this experiment. The best-fitting values of τ_h obtained with Eq. 12 and the fiber of Fig. 1 are plotted semilogarithmically versus the test membrane potential in Fig. 3 A. Experiments on other fibers show that τ_h as defined by Hodgkin and Huxley (1952) reaches a maximum of 30 ms near -75 mV. These experiments included standard double-

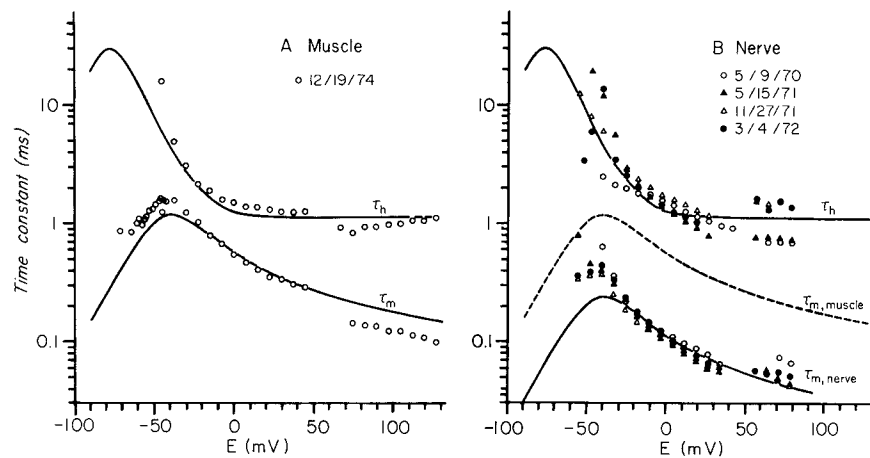


FIGURE 3. Observed and theoretical values of the time constants τ_m and τ_h in skeletal muscle and myelinated nerve at 5°C. The symbols are best-fitting values obtained for digitized experimental records using Eq. 12. (A) Time constants for muscle from the fiber used in Fig. 1. Solid lines are from the empirical theory developed in this paper. (B) Time constants for four nerve fibers studied at different times of year. Solid lines are from the theory for muscle in this paper except that τ_m for nerve is one-fifth of τ_m for muscle.

pulse sequences to follow the onset and recovery from inactivation at various potentials. As has been reported for axons (Armstrong, 1970; Goldman and Schaaf, 1973; Peganov, 1973; Peganov et al., 1973) the double-pulse experiments revealed a clear delay in the onset of sodium inactivation not contained in Eqs. 1–12. This complication is ignored in our empirical kinetic model for sodium permeability changes. The symbols in Fig. 3 A are the experimental points and the smooth curves are derived from the kinetic model.

The actual process of choosing empirical constants to fit Eqs. 10 and 11 to the observed values of τ_h and h_∞ was considerably simplified by the previous voltage clamp work on muscle. We made graphs of τ_h and h_∞ from the kinetic models (Table I) of Adrian et al. (1970) and of Ildefonse and Roy (1972) to compare with our results. For this purpose plotting the curve of time constants on a semilogarithmic plot as in Fig. 3 was very helpful, since rate differences due to differences of temperature could easily be taken into account by sliding the graphs vertically. Our measurements agreed most closely with the theory of Ildefonse and Roy with the simple modification of dividing their $\tilde{\alpha}_h$ and $\tilde{\beta}_h$ values (Table I) by 8.3. This change is equivalent to assuming a Q_{10} of 3.6 for α_h and β_h rate constants for a temperature change from 20–23°C to 5°C.

ACTIVATION OF NA CHANNELS Before the voltage dependence of m_∞ can be determined, the shape of the current-voltage relation I_{Na} of open sodium channels has to be measured. Two-step experiments to examine sodium “tail currents” at different potentials showed that the instantaneous sodium current-voltage relation is curved, so conductance and Ohm’s law cannot be used to describe currents in Na channels. In our fibers with ends cut in mixtures of CsF

TABLE I
PARAMETERS OF KINETIC MODELS FOR FROG SKELETAL MUSCLE AND
TWO GIANT AXONS

	Skeletal muscle			Giant axons	
	Ildefonso and Roy (1972) <i>R. esculenta</i>	Adrian et al. (1970) <i>R. temporaria</i>	This paper <i>R.</i> <i>pipiens</i>	Hodgkin and Hux- ley (1952)* <i>Loligo</i>	Goldman and Schauf (1973) <i>Myxicola</i>
	20-23°C	1-3°C	5°C	6.3°C	5°C
α_m (ms^{-1})	0.35	0.04	0.04	0.10	0.066
β_m (ms^{-1})	5.0	0.41	0.46	0.996	0.50
E_m (mV)	-57	-42	-42	-37	-45
V_{am} (mV)	5.0	10.0	10.0	10.0	5.95
$V_{\beta m}$ (mV)	13.7	18.0	18.0	18.0	23.8
α_h (ms^{-1})	0.001	0.003	0.00012	0.01	—
β_h (ms^{-1})	7.4	0.65	0.9	0.11	—
E_h (mV)	-25	-41	-25	-32	—
V_{oh} (mV)	11.0	14.7	11.0	20.0	—
$V_{\beta h}$ (mV)	13.6	7.6	13.6	10.0	—

* Parameters calculated by Adrian et al. (1970) assuming a resting potential for squid giant axons of -62 mV.

and NaF, the instantaneous current-voltage relation had the curvature of the Goldman (1943) and Hodgkin and Katz (1949) current equation, except that at high positive potentials the current was even smaller. For purely descriptive purposes we multiplied the Goldman-Hodgkin-Katz equation by an extra rectification factor W , giving

$$\bar{I}_{Na} = \bar{P}_{Na} [Na]_o \frac{F^2 E \exp [(E - E_{Na})F/RT] - 1}{RT \exp (EF/RT) - 1} \cdot W, \quad (13)$$

where W is

$$W = 0.6 + \frac{0.4}{1 + \exp [(E - 45)/10]}. \quad (14)$$

The factor W has less than 5% effect on sodium currents calculated at potentials more negative than +25 mV, and can be neglected for many purposes. In the rest of this paper wherever the symbol P_{Na} is used, it refers to the sodium permeability calculated with the standard Goldman-Hodgkin-Katz equation (Eq. 13 with $W = 1$).

The peak P_{Na} values for the fiber of Fig. 1 are plotted on a logarithmic scale versus potential in Fig. 2 B. As in other excitable systems, peak P_{Na} rises steeply for small depolarizations, increasing e -fold per 3.7 mV of depolarization, and levels off above 0 mV. The best values of τ_m obtained by fitting Eq. 1 to the currents in the same fiber are given in Fig. 3 A. The time constant reaches a maximum of 1.5 ms at -40 mV. Parameters needed to describe activation of Na channels can now be derived from the observations. As with inactivation, the work was simplified by comparison with existing kinetic models. Our τ_m - E curve and P_{Na} - E curve agreed most closely with the model of Adrian et al.

(1970). We used their empirical parameters (Table I) for Eqs. 6 and 7 with the slight modification of increasing $\tilde{\beta}_m$ by 15%. The smooth curve of τ_m in Fig. 3 A is calculated using these constants and the smooth P_{Na} - E curve in Fig. 2 B is calculated using our entire kinetic model with W given by Eq. 14.

KINETIC MODEL In summary our empirical kinetic model for currents in Na channels consists of the current expressions Eqs. 1, 13, and 14, the formulae for the rate of change of m and h Eqs. 2-3, and the formulae for the rate constants Eqs. 8-11 with their empirical coefficients found in Table I. These equations were used in the simulations of Figs. 10-12 of the first paper of this series (Hille and Campbell, 1976) as well as in drawing the curves of Figs. 2 and 3 in this paper. With these equations, taking $[Na]_o$ as 115 mM, E_{Na} as +63 mV, and \tilde{P}_{Na} as 15.7×10^{-4} cm/s gives a peak sodium current near -15 mV of 3.7 mA/cm² and a maximum sodium chord conductance near +15 mV of 57 mmho/cm². In fibers shortened to a sarcomere length of 1.6 μ m the values become 4.7 mA/cm² and 73 mmho/cm². These numbers are in accord with the average observed values of 4.7 mA/cm² and 75 mmho/cm² reported in Table I of the first paper. The simulations of that paper used a value of 14.7 instead of 15.7×10^{-4} cm/s for surface \tilde{P}_{Na} .

Kinetic Similarities Between Nerve and Muscle

There are two complete kinetic models for sodium currents at 20-22°C in myelinated nerve fibers, one for *Xenopus laevis* (Frankenhaeuser and Huxley, 1964) and the other for Eastern (Vermont) *Rana pipiens* (Dodge, 1961, 1963; modified by Hille, 1971 a). However, in our experience with several hundred myelinated fibers from *R. pipiens* studied at 5°C there are consistent differences from the existing models, so it seemed better to analyze some of these nerve fibers for comparison with muscle. The digitized current records (Hille, 1971 b) of four nerve fibers cut in KCl at 5°C were studied in detail by the methods already described for muscle. These records were selected because the fibers were under good voltage clamp control and gave currents with little ringing and low noise. Three fibers were from spring or winter Southwestern frogs (5/9/70, 11/27/71, and 3/4/72) and one from a spring Vermont frog (5/15/71). The type of frog seemed to make no systematic difference in the results. The external solution was the same as that used for the kinetic studies on muscle fiber.

A major ambiguity in interpreting studies with myelinated nerve fibers arises from the possibility of a significant DC offset between the potential reported by the apparatus and the actual membrane potential of the fiber. Some of the sources of the error are discussed in Hille (1971 b). Using the notation of Fig. 1 in Hille and Campbell (1976), the sources of offset and drift have been improved considerably since the earlier work of Frankenhaeuser and Dodge by the use of temperature-matched low input current transistors in amplifier A1, by cutting the nerve fiber in pool C to reduce R_{CD} , and by lengthening the BC seal to increase R_{BC} . An important criterion for choosing a holding potential has been to keep h_∞ in the range 0.5-0.7 so that Na channels are not strongly inactivated at rest. As is shown in Table II, the midpoint of the h_∞ curve recorded on nodes of

TABLE II
MIDPOINT POTENTIALS FOR h_{∞} AND m_{∞} IN EXCITABILITY MODELS FOR
NERVE AND MUSCLE

Membrane	E_H	$E_{h1/2}$	$E_{m1/2}$	Reference
	mV	mV	mV	
<i>Rana</i> muscle	-100	-68	-42	Adrian et al. (1970)
<i>Rana</i> muscle	-90	-79	-50	Ildefonse and Roy. (1972)
<i>Rana</i> muscle	-90	-79	-44	This paper
<i>Rana</i> node	-81	-78	-45	This paper
<i>Rana</i> node	-75	-75	-40	Dodge (1963)
<i>Xenopus</i> node	-70	-64	-36	Frankenhaeuser and Huxley (1964)
<i>Loligo</i> axon	-62*	-48	-37	Hodgkin and Huxley (1952)
<i>Myxicola</i> axon	-65	-49	-43	Goldman and Schauf (1973)

* Value given by Adrian et al. (1970).

E_H Holding potential of voltage clamp. E_H is considered to be equal to the normal resting potential except in work of Adrian et al. (1970).

$E_{h1/2}$ Midpoint potential of h_{∞} curve.

$E_{m1/2}$ Midpoint potential of m_{∞} curve.

Ranvier in our apparatus is 3 mV more negative than in the work of Dodge (1963) and 14 mV more negative than in the work of Frankenhaeuser. For this reason we believe that the resting potential of myelinated fibers is higher than in previous estimates, and in the following we assume without proof that our apparatus reports potentials correctly. The major remaining sources of error probably are junction potentials between KCl and the cut ends of the fiber, a junction potential in the BC seal and a current pathway between pools in the myelin and Schwann cell.

Using our values in Table II for the node of Ranvier, the midpoint potentials for h_{∞} and m_{∞} curves are the same in myelinated nerve as in skeletal muscle: Likewise the voltage dependence of the time constants τ_m and τ_h is similar between the two cell types. Fig. 3 B compares the best-fitting τ_m and τ_h values for the four nodes studied with the τ_m and τ_h curves of the muscle kinetic model already developed. The muscle theory for τ_h (solid line) agrees with the node observations without modification. The muscle theory for τ_m (dashed line) differs from the node observations, but can be brought into fair agreement by dividing the time constants by 5.0 to give the solid line. This is equivalent to multiplying $\bar{\alpha}_m$ and $\bar{\beta}_m$ for the muscle model by 5.0. To summarize, the time- and voltage-dependent features of gating in Na channels of frog node and frog skeletal muscle are nearly the same at 5°C except that activation processes in the node are five times faster.

Saxitoxin Blocks Na Channels of Nerve and Muscle Equally

The affinity of saxitoxin for its receptor on Na channels was measured by block of sodium permeability. To permit unambiguous comparison between muscle and nerve, the same solutions were applied at the same temperature (12°C) to semitendinosus muscle fibers and sciatic nerve fibers obtained from similar frogs in a 1-wk period. Concentrations of 0.5 nM and 2.0 nM saxitoxin were applied for 5 min and alternated with the control solution. The results are given in Table

TABLE III
BLOCK OF Na CHANNELS BY SAXITOXIN AT 12°C

	Nerve	Muscle
P_{Na} in 0.5 nM STX	0.80 ± 0.03 (6)	0.64 ± 0.03 (4)
P_{Na} in 2.0 nM STX	0.35 ± 0.03 (4)	0.31 ± 0.11 (2)
K_{STX}	1.3 nM (10)	0.88 nM (6)
K_{STX} 95% confidence interval	1.1 – 1.6 nM	0.61 – 1.3 nM

Best fit and confidence interval obtained from weighted sum of squared deviations from fit using the Patternsearch procedure as described in Colquhoun et al. (1974). P_{Na} expressed relative to the preceding control value and given as mean \pm SEM. Number of measurements in parentheses.

III as the ratio of sodium permeability at $E_M = 60$ – 70 mV during drug to that immediately before drug. The apparent drug dissociation constants K_{STX} are 1.3 nM for nerve and 0.88 nM for muscle with 95% confidence intervals of 1.1–1.6 and 0.61–1.3 nM. A two-tailed t test shows that the difference of the mean values for nerve and muscle is not significant at the $P = 0.05$ level. The rate of recovery from saxitoxin and tetrodotoxin block seemed slower with muscle than with nerve but this point was not studied quantitatively.

H⁺ and Ca⁺⁺ Ions Block and Shift

As has been reported for axons, the size of peak Na currents in muscle is reduced by raising the external H⁺ or Ca⁺⁺ concentration. We have analyzed the changes by the three-parameter model successfully used on the node of Ranvier (Woodhull, 1973). In this model the reduction of current is attributed to (a) a positive shift of the curve of peak sodium permeability P_{Na} on the voltage axis, specified by the single parameter, shift, and (b) a voltage-dependent reduction of peak P_{Na} due to blocking of Na channels by bound H⁺ or Ca⁺⁺ ions. The binding is described by a conventional bimolecular adsorption isotherm with a two-parameter apparent dissociation constant $K_{diss}(E)$ given by

$$K_{diss}(E) = K_{diss}(0) \exp\left(\frac{z\delta FE}{RT}\right), \quad (15)$$

where E is the membrane potential, z is the charge of the blocking ion, RT/F is 24.0 mV at 5°C, and δ is a coefficient between 0 and 1 expressing the fraction of the membrane potential drop affecting the binding of the ion. The parameters $K_{diss}(0)$ and δ are chosen from the change of shape of the peak P_{Na} - E curves, and the shift is measured relative to the control P_{Na} - E curve when shape changes have been accounted for.

Fig. 4 shows peak P_{Na} - E curves measured at pH 7.4, 6, 5.2, and 4.5 and plotted semilogarithmically. As with nerve, lowering the pH depresses P_{Na} , shifts the curves to the right, and changes their shape. The points are experimental observations, and the smooth curves show a fit obtained with Woodhull's three-parameter model. The lines were drawn from an arbitrary function drawn through the points at pH 7.4. For other pH values the function was shifted on the voltage axis and then multiplied by the expected fraction of channels not

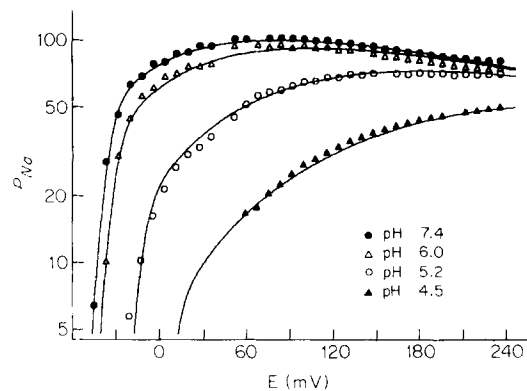


FIGURE 4. Block of Na channels and shift of their voltage dependence at low pH. Symbols are observed peak P_{Na} for voltage clamp steps to the potential E after a conditioning prepulse to -135 mV. Fiber ends cut in 115 mM CsF + 5 mM NaF. Temperatures 5°C . Smooth line for pH 7.4 is drawn by computer from a fitted arbitrary function. Other smooth lines are drawn from the line for pH 7.4 transformed according to the three-parameter theory given in the text with $\delta = 0.27$, $\text{p}K_a = 5.35$, and shifts of 4.5 , 14.7 , and 46.0 mV.

blocked by a proton at each voltage assuming that $\text{p}K_a(0)$ is 5.35 and δ is 0.27 . The agreement of experiment and model is very close. The mean value of the fitted $\text{p}K_a(0)$ on seven different muscle fibers was 5.33 ± 0.03 (SEM). A value of 0.27 for δ gave the best fit in all cases, while values as high as 0.29 or as low as 0.25 gave quite noticeable deviations from the observations. The experimental voltage shift may be defined as the shift required to bring the pH 7.4 curve into register with the observations at another pH, taking a rightward movement in Fig. 4 as a positive shift. The mean values obtained are summarized in Table IV. As in the experiment of Fig. 4, the tiny sodium currents below E_{Na} at pH 4.2 could not be resolved in the photographs taken so shifts could not be computed. With two fibers however, the current was filtered by a low pass filter and observed at higher gain than usual, and more care was taken to balance the leak subtracting circuit. Three shifts from these two fibers are averaged in Table IV, but because of the scatter and small signal size the results are not very reliable. The results with muscle are plotted for comparison with curves obtained with myelinated fibers in Fig. 5. A qualitative similarity of the pH effects is evident and is discussed in more detail later.

Fig. 6 is a semilogarithmic plot of peak P_{Na} - E curves measured at 0 , 0.5 , 2 , 5 , and 20 mM Ca^{++} and pH 7.4. The most prominent change as Ca^{++} concentration is increased is a rightward shift of the curves to more positive voltages. As with pH changes, the smooth curves have been fitted using the three-parameter theory although in this example voltage-dependent block is hardly evident. Values of 80 mM Ca^{++} for $K_{\text{diss}}(0)$ and 0.27 for δ have been assumed. They account for the small depression of permeability seen in 20 mM Ca^{++} but cannot be regarded as well determined. The mean shifts relative to control curve at 2 mM Ca^{++} are summarized in Table IV and plotted for comparison with results on myelinated fibers in Fig. 5. The calcium-dependent shifts with frog muscle

TABLE IV
SHIFTS OF THE $P_{Na} - E$ CURVE WITH pH AND Ca^{++}

pH changes		[Ca^{++}] changes	
pH	Shift mV	[Ca^{++}] mV	Shift mV
4.5	44.7 ± 5.4 (3)	0	-15.0 ± 0.9 (8)
5.2	15.5 ± 2.0 (7)	0.5	-9.0 ± 1.0 (9)
6.0	4.8 ± 1.3 (6)	5	8.4 ± 0.6 (6)
9.4	-3.2 ± 1.1 (5)	20	19.4 ± 2.4 (6)

Shifts measured relative to pH 7.4 and 2 mM Ca^{++} and given as mean \pm SEM with number of observations in parentheses.

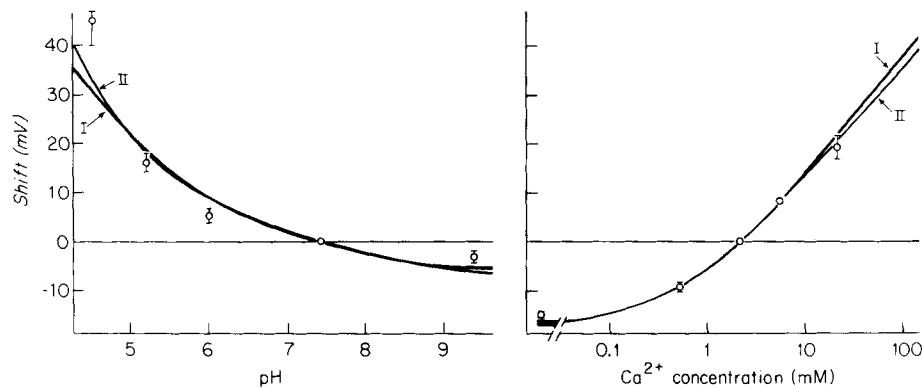


FIGURE 5. Comparison of pH and Ca dependence of shifts in muscle and nerve. The observations on muscle in Table IV are shown as circles with error bars of ± 1.0 SEM. The smooth curves are taken from Figs. 1, 2, 5, and 6 of Hille et al. (1975). They approximate the pH and Ca dependence of shifts in myelinated nerve and are derived from two specific Gouy-Chapman-Stern surface charge models. Model I has a surface potential of -90.6 mV in standard Ringer solution and model II, a potential of -64.3 mV.

are not significantly different from shifts with frog nerve. In summary, Na channels of muscle and nerve are blocked equally by hydrogen ions and their voltage-sensing mechanisms are biased equally by changes of external pH or calcium concentration.

DISCUSSION

Comparison with Other Kinetic Models

There are now several kinetic models for Na channels of axons and muscle fibers. The kinetic constants for those models with equations in the same form as Eqs. 8-11 are listed in Table I. Such numbers are difficult to interpret by themselves, so the curves for τ_m , τ_h , m_∞ , and h_∞ were calculated from all the models in the literature and compared graphically. Table II lists the calculated midpoint potentials for the m_∞ and h_∞ curves, and Fig. 7 shows the τ_m and τ_h curves of all the models in the voltage range from -60 to $+75$ mV where the time

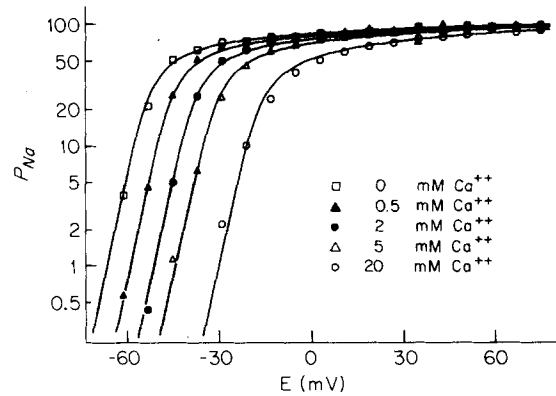


FIGURE 6. Shift of the voltage dependence of opening of Na channels by Ca^{++} changes. Symbols are observed peak P_{Na} for voltage clamp steps to the potential E after a conditioning prepulse to -135 mV. Same muscle fiber as in Fig. 6. Smooth line for 2 mM Ca^{++} arbitrary. Other lines calculated from the three-parameter theory given in text with $\delta = 0.27$, $K_{\text{Ca}} = 80$ mM, and shifts of -14.4 , -7.8 , 7.9 , and 18.0 mV relative to the control.

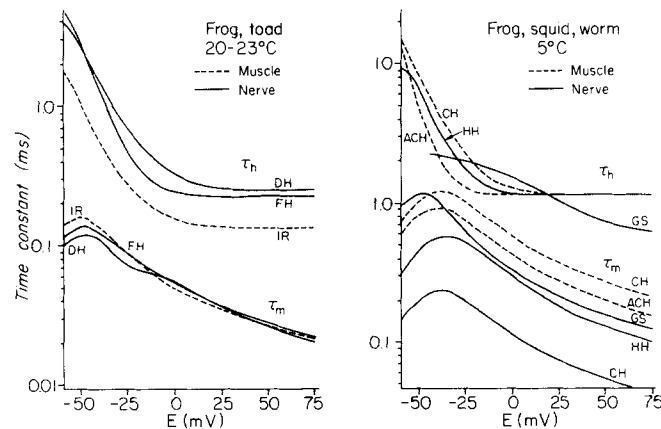


FIGURE 7. Comparison of the voltage dependence of τ_m and τ_h in all existing empirical kinetic models for Na channels of muscle and nerves. The models shown for 5°C were actually from the range of temperatures 1 – 6.3°C and were scaled using a Q_{10} of 3.0 for rate constants before plotting. References: DH, *R. pipiens* (Dodge, 1961, 1963; as modified by Hille, 1971 a); FH, *X. laevis* (Frankenhaeuser and Huxley, 1964); IR, *Rana esculenta* (Ildefonse and Roy, 1972); CH, *R. pipiens* muscle and nerve (Campbell and Hille, this paper); HH, *Loligo forbesi* (Hodgkin and Huxley, 1952); ACH, *Rana temporaria* (Adrian et al., 1970); GS, *Myxicola infundibulum* (Goldman and Schaaf, 1973). The τ_h curve for nerve at 5°C (this paper) is the same as the dashed curve CH for muscle.

constants can be obtained from single-step depolarizations using Eq. 12. One panel shows unscaled curves for 20 – 23°C and the other shows models for 1 – 6.3°C but all scaled to 5°C assuming a Q_{10} of 3.0 for the rate constants.

If all the curves are fair descriptions of Na channels in the different prepara-

tions, the following list of conclusions may be drawn. The gating mechanism of Na channels has strong similarities in all systems studied. Nodes of *Xenopus* and *Rana* are virtually the same at 20–23°C. In frog nerve the Q_{10} for τ_h is 2.8 and for τ_m , 1.6 (comparing curves DH and FH with curves CH for nerve), in agreement with Frankenhaeuser and Moore (1963). In frog muscle the Q_{10} , however, is 4 for both τ_m and τ_h (comparing curves IR with curves ACH and CH for muscle). At low temperature, myelinated nerve has the fastest activation, perhaps to take advantage of the very short membrane time constant ($R_M C_M$) of this tissue. In all axons the ratio τ_h/τ_m is significantly larger than in frog muscle, which has the consequence that in the muscle model the peak sodium permeability P_{Na} may reach only 20–30% of the hypothetical limiting value of \bar{P}_{Na} whereas in nerve the value is closer to 50–60%. It is of general theoretical interest to know if membranes actually have enough Na channels to give the full \bar{P}_{Na} since that would bear on the physical interpretation of expressions like m^3h . Experiments to increase peak P_{Na} by blocking inactivation in axons have not succeeded (Hille, 1976), but the low τ_h/τ_m ratio in muscle makes it worthwhile to try these experiments again there.

Common Features of Na Channels in the Frog

Although we are still far from understanding how Na channels work, several features in addition to gating kinetics have been investigated extensively. In the frog node of Ranvier the most explored regions of the channel are the ionic selectivity filter within the pore and a region of fixed negative charge on the external membrane surface overlying the voltage-sensing mechanism(s). The neighborhood of the selectivity filter is thought to include an essential ionized acid group (Hille, 1975 *a*) and a critical array of hydrogen bond acceptors forming a narrow slit that permeant ions must pass through. The outer end of the selectivity filter may also form the receptor for toxins like tetrodotoxin and saxitoxin (Hille, 1975 *b*). The experiments in this paper show that the pK_a and effective electrical distance in the membrane to the essential acid group is the same in frog muscle as it is in frog nerve. In addition the affinity of saxitoxin for its receptor is the same, and the experiments in the previous paper (Campbell, 1976) show that the ionic selectivity is basically the same. Finally the current-voltage relation of open channels I_{Na} fits the Goldman-Hodgkin-Katz equation in both types of cells. All of these measurements are sensitive tests of the similarity of the conducting region of the channel. They argue for a virtual molecular identity of the narrow part of the open pore in nerve and skeletal muscle.

The region of negative fixed charge on the outer surface of the membrane can be explored by measuring shifts of the voltage dependence of gating as the external pH, divalent ions, or monovalent ions are changed. Hille et al. (1975) measured shifts of the P_{Na} - E curve of the node of Ranvier and give an extensive quantitative description in terms of combinations of dissociable groups on the membrane. Complete agreement of the muscle observations with the nerve theory might not be expected because activation and inactivation make different relative contributions to the P_{Na} - E curves in nerve and muscle and, at least in nerve, shifts of inactivation and activation are not equal. Nevertheless from the comparison of the theoretical lines with observations on muscle in Fig. 5, it is

evident that the surface density and dissociation constants of the fixed charges may be the same in nerve and muscle. Unfortunately as is explained in Hille et al. (1975) even such relatively elaborate experiments are not sufficient to permit an unambiguous choice of surface charge density or dissociation constants. Many surface charge models will fit, two of which are given in the figure. Costantin (1968) measured shifts of what he called sodium conductance threshold with a two-microelectrode point clamp on frog skeletal muscle. The methods differ enough so that complete quantitative agreement is not expected, but he found a 30-mV shift on changing from 0.2 mM to 10 mM Ca^{++} . As in frog nerve Costantin found that equimolar replacement of Mg^{++} for Ca^{++} resulted in a negative shift.

In conclusion Na channels of frog nerve and muscle are nearly indistinguishable by most known criteria. The negative charge and shape of the selectivity filter and toxin receptor are similar. The barriers to ion flow in the pore are similar. The electrostatic effects and dissociation constants of external charges seen by the voltage sensors are similar. The voltage dependence of gating is similar. The only real area of difference detected is that the Q_{10} and actual rates of gating are different in nerve and muscle. These observations could be understood if all the molecules making the pore, gates, and sensors were identical in the two excitable cells but the surrounding membrane material were different enough to give different energy barriers for the various conformational changes underlying sensing and gating. Despite their proposed identity, the Na channels of nerve and muscle are probably found at different average densities in the excitable membrane. Frankenhaeuser and Huxley (1964) use a \bar{P}_{Na} value of 80×10^{-4} cm/s in their model for myelinated fibers, to be compared with our value of 15.7×10^{-4} cm/s for muscle.

We thank Susan Morton for invaluable secretarial help, S. Y. Chiu for help with data analysis, Perry Johnson for building apparatus, Dr. D. Colquhoun for advice on curve-fitting procedures, Dr. W. Almers for reading the manuscript, and Dr. T. H. Kehl and his staff for conceiving and programming the new minicomputer.

Supported by grants NS 08174, NS 05082, GM 00260, and FR 00374 from the National Institutes of Health.

Received for publication 7 July 1975.

REFERENCES

- ADRIAN, R. H., W. K. CHANDLER, and A. L. HODGKIN, 1970. Voltage clamp experiments in striated muscle fibres. *J. Physiol. (Lond.)*, **208**:607-644.
- ARMSTRONG, C. M., 1970. Comparison of g_{K} inactivation caused by quaternary ammonium ion with g_{Na} inactivation. *Biophys. Soc. Annu. Meet. Abstr.*, **14**:185a.
- CAMPBELL, D. T., 1976. Ionic selectivity of the sodium channel of frog skeletal muscle. *J. Gen. Physiol.*, **67**:295-307.
- COLQUHOUN, D., 1971. Lectures on Biostatistics. Clarendon Press, Oxford.
- COLQUHOUN, D., H. P. RANG, and J. M. RITCHIE, 1974. The binding of tetrodotoxin and α -bungarotoxin to normal and denervated mammalian muscle. *J. Physiol. (Lond.)*, **240**:199-226.
- COSTANTIN, L. L., 1968. The effect of calcium on contraction and conductance thresholds in frog skeletal muscle. *J. Physiol. (Lond.)*, **195**:119-132.
- DODGE, F. A., 1961. Ionic permeability changes underlying nerve excitation. In *Biophysics*

- of Physiological and Pharmacological Actions. AAAS, Washington, D.C.
- DODGE, F. A., 1963. A study of ionic permeability changes underlying excitation in myelinated nerve fibers of the frog. Ph.D. Thesis. The Rockefeller University, New York. Microfilm 64-7333, University Microfilms, Ann Arbor, Mich.
- FRANKENHAEUSER, B., and A. F. HUXLEY, 1964. The action potential in the myelinated nerve fibre of *Xenopus laevis* as computed on the basis of voltage clamp data. *J. Physiol. (Lond.)*, **171**:302-315.
- FRANKENHAEUSER, B., and L. E. MOORE, 1963. The effect of temperature on the sodium and potassium permeability changes in myelinated nerve fibres of *Xenopus laevis*. *J. Physiol. (Lond.)*, **169**:431-437.
- GOLDMAN, D. E., 1943. Potential, impedance, and rectification in membranes. *J. Gen. Physiol.* **27**:37-60.
- GOLDMAN, L., and C. L. SCHAUF, 1973. Quantitative description of sodium and potassium currents and computed action potentials in *Myxicola* giant axons. *J. Gen. Physiol.* **61**:361-384.
- HILLE, B., 1971 *a*. Voltage clamp studies on myelinated nerve fibers. In *Biophysics and Physiology of Excitable Membranes*. W. J. Adelman, editor. Van Nostrand-Reinhold, New York. 230-246.
- HILLE, B., 1971 *b*. The permeability of the sodium channel to organic cations in myelinated nerve. *J. Gen. Physiol.* **58**:599-619.
- HILLE, B., 1975 *a*. An essential ionized acid group in sodium channels. *Fed. Proc.* **34**:1318-1321.
- HILLE, B., 1975 *b*. The receptor for tetrodotoxin and saxitoxin: a structural hypothesis. *Biophys. J.* **15**:615-619.
- HILLE, B., 1976. Gating in sodium channels of nerve. *Annu. Rev. Physiol.* In press.
- HILLE, B., and D. T. CAMPBELL, 1976. An improved Vaseline gap voltage clamp for skeletal muscle fibers. *J. Gen. Physiol.* **67**:265-293.
- HILLE, B., A. M. WOODHULL, and B. I. SHAPIRO, 1975. Negative surface charge near sodium channels of nerve: Divalent ions, monovalent ions, and pH. *Philos. Trans. R. Soc. Lond. B Biol. Sci.* **270**:301-318.
- HODGKIN, A. L., and A. F. HUXLEY, 1952. A quantitative description of membrane current and its application to conduction and excitation in nerve. *J. Physiol. (Lond.)*, **117**:500-544.
- HODGKIN, A. L., and B. KATZ, 1949. The effect of sodium ions on the electrical activity of the giant axon of the squid. *J. Physiol. (Lond.)*, **108**:37-77.
- ILDEFONSE, M., and G. ROY, 1972. Kinetic properties of the sodium current in striated muscle fibres on the basis of the Hodgkin-Huxley theory. *J. Physiol. (Lond.)*, **227**:419-431.
- KEHL, T. H., C. MOSS, and L. DUNKEL, 1975. LM²-A logic machine mini-computer. *Computer*, **8**:12-22.
- PEGANOV, E. M., 1973. Kinetics of the process of inactivation of sodium channels in the node of Ranvier of frogs. *Bull. Exp. Biol. Med. (Engl. Transl. Byull. Eksp. Biol. Med.)*, **11**:5-9.
- PEGANOV, E. M., E. N. TIMIN, and B. I. KHODOROV, 1973. Interrelationship between the processes of sodium activation and inactivation. *Bull. Exp. Biol. Med. (Engl. Transl. Byull. Eksp. Biol. Med.)*, **10**:7-11.
- WOODHULL, A. M., 1973. Ionic blockage of sodium channels in nerve. *J. Gen. Physiol.* **61**:687-708.